Maximum Power Point Tracking of Grid Connected Photovoltaic System Employing Model Predictive Control

Mohammad B. Shadmand[1], *Student Member, IEEE*, Mostafa Mosa[2], *Student Member, IEEE*, Robert S. Balog[3], *Senior Member, IEEE*, and Haitham Abu Rub[4], *Senior Member, IEEE*
Renewable Energy & Advanced Power Electronics Research Laboratory, Dept of Electrical & Computer Engineering, Texas A&M University, College Station, USA[1,2,&3]
Dept of Electrical & Computer Engineering, Texas A&M University at Qatar, Doha, Qatar[4]
mohamadshadmand@gmail.com[1], m.mosa@ieee.org[2], robert.balog@ieee.org[3], haitham.abu-rub@qatar.tamu.edu[4]

***Abstract* — This paper presents a maximum power point tracking (MPPT) technique using model predictive control (MPC) for single phase grid connected photovoltaic (PV) systems. The technique exhibits fast convergence, which is ideal for rapidly varying environmental conditions such as changing temperature or insolation or changes in morphology of the PV array itself. The maximum power of PV system is tracked by a high gain DC-DC converter and feeds to the grid through a seven-level inverter. Considering the stochastic behavior of the solar energy resources and the low conversion efficiency of PV cells, operation at the maximum possible power point is necessary to make the system economical. The main contribution of this paper is the development of incremental conductance (INC) method using two-step model predictive control. The multilevel inverter controller is based on fixed step current predictive control with small ripples and low total harmonic distortion (THD). The proposed MPC method for the grid connected PV system speeds up the control loop by sampling and predicting the error two steps before the switching signal is applied. As a result, more energy will be captured from the PV system and injected into grid particularly during partially cloudy sky. A comparison of the developed MPPT technique to the conventional INC method shows significant improvement in dynamic performance of the PV system. Implementation of the proposed predictive control is presented using the dSPACE DS1103.**

I. Introduction

With the depletion of fossil fuels and skyrocketing levels of CO_2 in the atmosphere, renewable energy sources continue to gain popularity as a long-term sustainable energy source. Reduction in the cost of photovoltaic cells has increased the interest in using this renewable energy source. The 60% annual growth in the installed capacity of photovoltaic (PV) systems from 2004 to 2009, and 80% in 2011 reveals the fact of their popularity as a sustainable energy sources [1, 2].

Due to high variability of solar energy resources [3-5], maximum power point tracking (MPPT) is required to ensure continuous operation of the Photovoltaic (PV) system at the maximum power point [6-11]. Stochastic mathematical models and hourly-data driven models do not adequately reflect the true nature of power variability which becomes more readily apparent when samples at high-temporal resolution, such as 10 second intervals, as illustrated in Fig. 1 which reveals higher ramp-rates than predicted using other lower-fidelity and stochastic models. This fact necessitates the MPPT procedure to track fast ramp-rates. Insolation conditions can also change quickly when considering non-planar PV surfaces that are morphing shape and changing view factor with respect to the incident solar radiation [12-14], thus requiring fast MPPT convergence.

Many MPPT methods have been suggested over the past few decades; the relative merits of these various approaches are discussed in [7]. The critical operating regime is low insolation. Capturing all of the available solar power during low insolation periods can substantially improve system performance. An effective MPPT controller and converter can use available energy to significantly reduce the amount of installed PV.

Considering the MPPT techniques listed in [7], candidate techniques include Incremental Conductance (INC) [6], Perturb-and-Observe (P&O) [15], fractional Open-Circuit Voltage (Voc) [16], and Best Fixed Voltage (BFV) [4]. Each approach has certain advantages and disadvantages for the present application. INC is a well-known technique with relatively good performance; however, the INC method does not guarantee converge to the true maximum power point. Also, in practice INC is relatively slow, and that limits its ability to track fast transient insolation conditions.

The PV array can feed power to the grid through a DC/DC converter boosting the output voltage and a grid connected inverter [17-24]. The main contribution of this paper is the

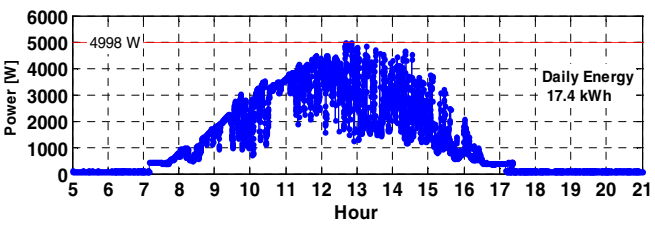

Fig. 1: Output power of a PV array installed at Texas A&M University during a partially cloudy day.

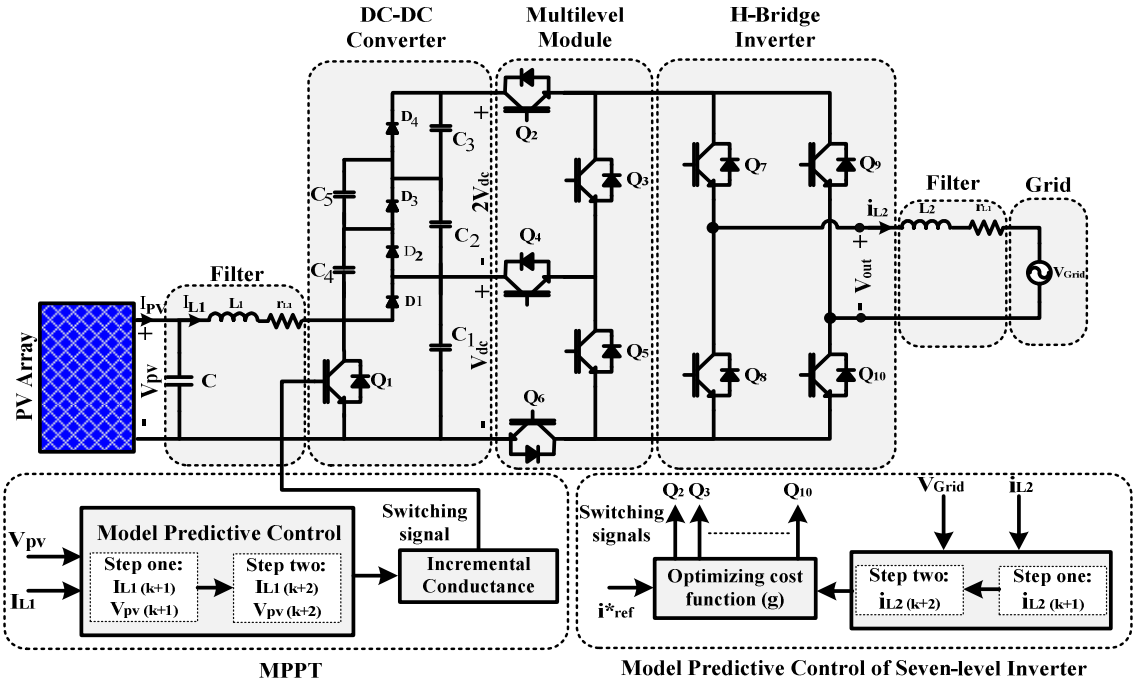

Fig. 2: General schematic of the system and proposed model predictive control for grid connected PV system.

development of the INC method using a two-step model predictive control for a multilevel boost DC-DC converter. The boost converter output power is fed to the ac grid through a seven level inverter controlled by model based current predictive method. By predicting the future behavior of the PV system, the proposed MPC method in an elegant, embedded controller that has faster response than the conventional INC technique under rapidly changing atmospheric conditions without requiring expensive sensing and communications equipment and networks to directly measure the changing solar insolation.

II. Description of Complete System

Fig. 2 illustrates the general schematic of the complete grid connected photovoltaic system controlled by predictive methods. As it is shown, the system contains a multilevel DC-DC boost converter to extract the maximum power from the PV arrays and to feed it into the grid through a seven level inverter. Since only one switch is used in the selected multilevel boost DC-DC converter topology, the control procedure is simpler than other topologies such as the switched capacitor converter with a boost stage [25]. The output voltage of the DC-DC converter is proportional to the number of levels, which can be increased by adding two additional capacitors and diodes.

The DC-DC converter in this paper has three levels. At the dc-link stage of the system, if the average voltage across the capacitor C_1 is V_{dc}, then the average voltage across capacitors C_2 and C_3 together will be $2V_{dc}$. The detail mode of operation of this DC-DC converter with two levels is presented in [10], this concept can be extended for the three levels topology presented in this paper.

The seven level inverter topology used to feed power to the grid can be divided into two parts: multilevel module and H-bridge inverter. The multilevel module is cascaded with an H-Bridge inverter operating at low frequency to reduce the switching losses. Table 1 demonstrates the summary of the output voltage levels as a function of switching states. The state of the switches can be represented by 0 and 1, where state 0 means the switch is OFF, and state 1 means the switch is ON.

III. Principle of Model Predictive Control

Application of Model Predictive Control (MPC) in power electronics with low switching frequency comes back to 1980's for high power applications [26, 27]. Since high switching frequencies for the MPC algorithm required large

Table 1: Summary of output voltage levels as function of switching states.

Output Voltage (V_{out})	Multilevel Inverter Switches States								
	Q_2	Q_3	Q_4	Q_5	Q_6	Q_7	Q_8	Q_9	Q_{10}
$+3V_{dc}$	1	0	0	0	1	1	0	0	1
$+2V_{dc}$	1	0	1	1	0	1	0	0	1
$+V_{dc}$	0	1	1	0	1	1	0	0	1
0	0	1	0	1	0	1	0	0	1
$-V_{dc}$	0	1	1	0	1	0	1	1	0
$-2V_{dc}$	1	0	1	1	0	0	1	1	0
$-3V_{dc}$	1	0	0	0	1	0	1	1	0

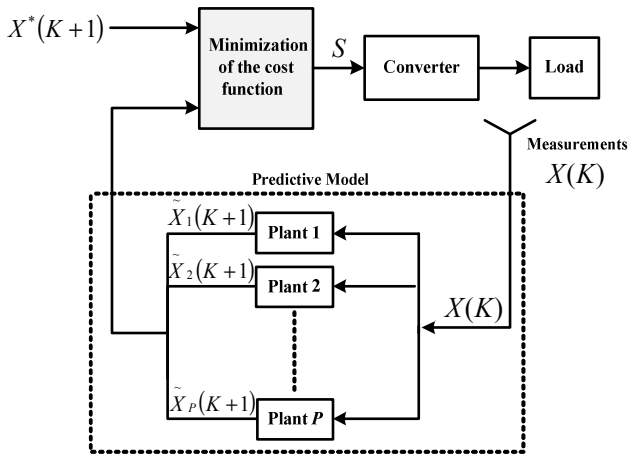

Fig. 3: MPC general schematic for power electronics converters.

calculation time, it was not feasible at that time which prevented widespread adoption. In the past decade, by improvement of high speed microprocessors, interest in the application of MPC in power electronics with high switching frequency has been increased considerably [10, 28-31].

The main characteristic of MPC is predicting the future behavior of the desired control variables [27, 28] until a specific time in horizon. The predicted control variables will be used to obtain the optimal switching state by minimizing a cost function. The discrete time model of the control variables will be used for prediction which can be presented as state space model as follow [27]:

$$x(k+1) = Ax(k) + Bu(k) \tag{1}$$

$$y(k) = Cx(k) + Du(k) \tag{2}$$

Then a cost function that takes into consideration the future states, references and future actuations can be defined [27]:

$$g = f(x(k), u(k), \cdots, u(k+N)) \tag{3}$$

The defined cost function g should be minimized for a predefined horizon in time N; a sequence of N optimal actuations will be determined where the controller only applies the first element of sequence:

$$u(k) = [1 \quad 0 \quad \cdots \quad 0] \arg \min_{u} g \tag{4}$$

At each sampling time the optimization problem is solved again by using new set of measured data to obtain a new sequence of optimal actuation. The MPC for power electronics converters can be designed using the following steps [28]:

- Determination of power converter model which specify the input-output relation of the voltages and currents.
- Determination of discrete-time model of the control variables for predicting their future behavior.
- Designing the cost function, subject to minimization, which demonstrates the preferred behavior of the power converter.

The general scheme of MPC for power electronics converters is illustrated in Fig. 3 [28]. In this block diagram, measured variables $X(K)$ are used in the model to estimate predictions $\tilde{X}(K+1)$ of the controlled variables for all of the p possible switching states (plants), where $p \in \{1 \cdots P\}$ for P possible resulting circuit configurations (plants). These predictions are then evaluated using a cost function which compares them to the reference values $X^*(K+1)$ by considering the design constraints. Finally the optimal actuation S is selected and applied in the converter. The general form of the cost function g subject to minimization can be formulated as

$$g = \left|X_1^*(K+1) - \tilde{X}_1(K+1)\right| + \lambda_1 \left|X_2^*(K+1) - \tilde{X}_2(K+1)\right| + \ldots + \lambda_P \left|X_P^*(K+1) - \tilde{X}_P(K+1)\right| \tag{5}$$

where λ is the value or weight factor for each objective.

The schematic of Fig. 3 is comprehensive and can be applied to any power converter topology and number of phases as well as the generic load illustrated in Fig. 3 which can represent the power grid or any other active or passive load. In this paper the multilevel boost DC-DC converter and multilevel grid connected inverter as illustrated in Fig. 1 has been used as power conversion stage.

IV. Model Predictive Control of the System

A. Predictive Maximum Power Point Tracking

The discrete time model of the DC-DC converter is used to determine predicted control variables:

$$I_{L1}(K+n+1) = I_{L1}(K+n)\left[1 - r_{L1} \times \frac{T_s}{L_1}\right] + V_{PV}(K) \times \frac{T_s}{L_1} - (1-S) \times V_C(K+n) \tag{6}$$

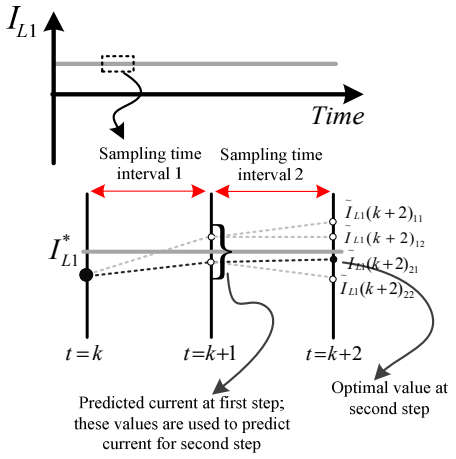

Fig. 4: Prediction of PV array side current observation.

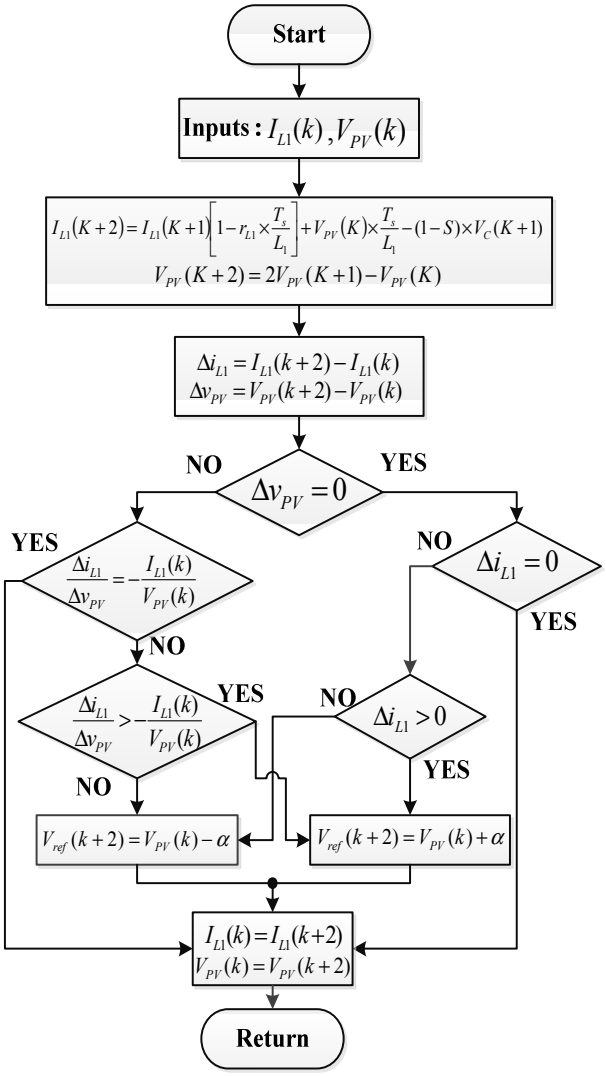

Fig. 5: MPC maximum power point tracking procedure.

$$V_{PV}(K+n+1)=V_{PV}(K)+\left[I_{PV}(K+n)-I_{L1}(K+n)\right]\times\frac{T_s}{C} \tag{7}$$

where n+1 is the number of steps in the future being predicted at the current K^{th} step; S is 1 when the switch is ON and 0 when the switch is OFF; and T_S is the sampling time. In this paper the control variables predicted two steps in horizon. Equations (6) and (7) have four inputs I_{L1}, V_{pv}, I_{pv}, and V_C. In order to reduce the number of sensors, these equations can be rearranged by decreasing the number of input variables. Thus (7) can be represented as

$$V_{PV}(K+2)=2V_{PV}(K+1)-V_{PV}(K) \tag{8}$$

In order to calculate the value of control variables at time K+2, the estimated value of the current of the inductor, L_1, and PV voltage at time K+1 are used. Thus at sampling time K+2, four values for control variables are predicted and the optimum value will be selected as illustrated graphically in

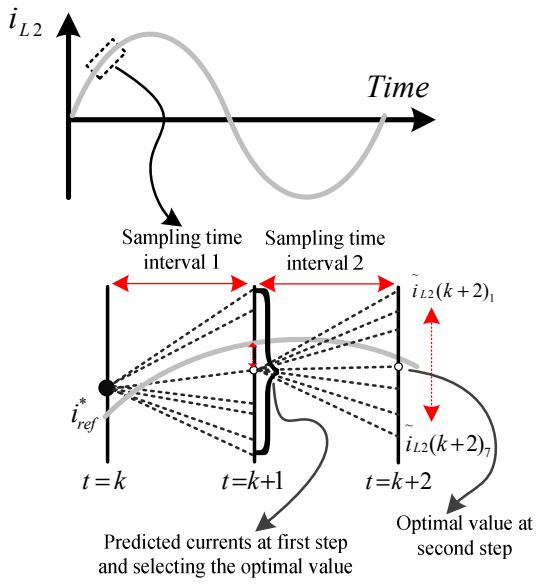

Fig. 6: Prediction of grid side current observation.

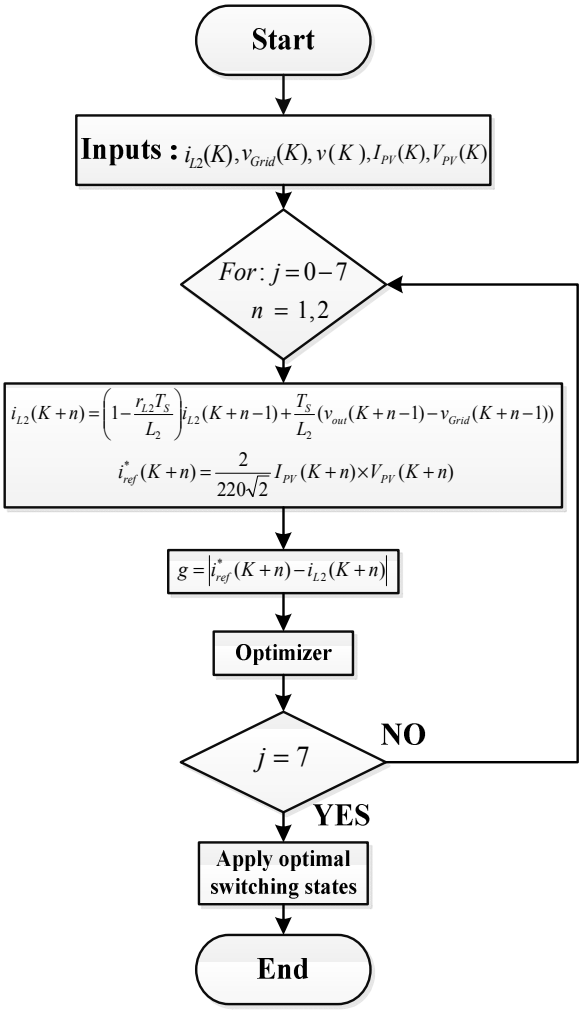

Fig. 7: Model predictive control of the multilevel inverter.

Fig. 4. The derived equations can be expressed in matrix form by (9) and (10) when the switch is ON and OFF respectively

$$\begin{bmatrix} I_{L1}(K+2) \\ V_{PV}(K+2) \end{bmatrix} = \begin{bmatrix} 1-r_{L1}\times\frac{T_s}{L_1} & \frac{T_s}{L_1} \\ 0 & 2 \end{bmatrix} \times \begin{bmatrix} I_{L1}(K+1) \\ V_{PV}(K+1) \end{bmatrix} + \begin{bmatrix} 0 \\ -1 \end{bmatrix} \times V_{PV}(K) \quad (9)$$

$$\begin{bmatrix} I_{L1}(K+2) \\ V_{PV}(K+2) \end{bmatrix} = \begin{bmatrix} 1 & 0 \\ 0 & 2 \end{bmatrix} \times \begin{bmatrix} I_{L1}(K+1) \\ V_{PV}(K+1) \end{bmatrix} + \begin{bmatrix} 0 \\ -1 \end{bmatrix} \times V_{PV}(K) \quad (10)$$

The summary of the proposed MPPT algorithm is illustrated in Fig. 5.

B. Predictive Current Control

The next step is the current predictive control of the multilevel inverter. The load current in continuous form can be determined using the following expression

$$v_{out} = L_2 \frac{di_{L2}}{dt} + r_{L2} i_{L2} + v_{Grid} \quad (11)$$

By using the Euler forward method, the derivative in (11) can be approximately discretize as

$$L_2 \frac{di_{L2}}{dt} = L \frac{i_{L2}(K+1) - i_{L2}(K)}{T_s} \quad (12)$$

where T_s is the sampling period. Based on (11) and (12) the load side current can be predicted for n steps in horizon of time by using

$$i_{L2}(K+n) = \left[1 - \frac{r_{L2}T_S}{L_2}\right] i_{L2}(K+n-1) + \frac{T_S}{L_2}(v_{out}(K+n-1) - v_{Grid}(K+n-1)) \quad (13)$$

where $i_{L2}(K+n)$ is the predicted value of the grid side current at time $K+n$. In this paper, i_{L2} is predicted two steps, $n=2$, into the horizon of time as illustrated in Fig. 6. The reference current to be tracked and the cost function, g, is given by

$$i^*_{ref}(K+n) = \frac{2}{220\sqrt{2}} I_{PV}(K+n) \times V_{PV}(K+n) \quad (14)$$

$$g = \left| i^*_{ref}(K+n) - i_{L2}(K+n) \right| \quad (15)$$

The cost function needs to be minimized by evaluating all of the possible switching states presented in Table 1 for each step. The summary of optimal switching state selection procedure is illustrated in Fig. 7.

V. Results and Discussion

The proposed controller for the PV system is modeled in MATLAB-Simulink, and implemented in dSPACE DS1103. The I-V and P-V characteristics of the PV system for different irradiance levels are illustrated in Fig. 8. The SUNPOWER SPR-305-WHT is used as PV module type. The PV module characteristics under standard test condition (STC: solar irradiance = 1 kW/m^2, cell temperature = 25 deg. C) are:

- Open circuit voltage (Voc) = 64.2 V
- Short-circuit current (Isc) = 5.96 A
- Voltage at MPP (VMP) = 54.7 V
- Current at MPP (IMP) = 5.58 A

The sampling time, T_s, is 10 µs. In this paper the MPC for MPPT is compared to the commonly used incremental conductance method. Fig. 9 illustrates the simulation results of the proposed MPC and INC method. As it is shown the MPPT is enabled at time 0.1 s, the irradiance decreases gradually at time 0.3 s from 1250 W/m^2 to 1000 W/m^2, and finally there is a step change in irradiance level at time 0.6 s from 1000 W/m^2 to 1250 W/m^2. By comparing Fig. 9 (d) and (g) to (i) and (h) respectively, it can be noticed that the maximum power is tracked much faster when using two steps in MPC-MPPT than the conventional INC-MPPT method. The maximum power point when using two steps MPC-MPPT is achieved 1 ms after the step change in solar irradiance occurred. Conversely it is about 4 ms for conventional INC-MPPT. By considering continuous operation of the PV systems over the year, the extra amount of energy captured by the proposed MPPT technique is significant, particularly under the cloudy sky condition such as solar irradiance level of Fig. 1.

The simulation results of the grid side voltage and current, using MPC for the multilevel inverter, is illustrated in Fig. 10. Fig. 10 (a) and (c) show that the unity power factor is achieved and that the controller response to the step change in solar irradiance level at time 0.6 s is very fast.

The simulation results are validated experimentally by real-time implementation of the control strategy with dSPACE DS1103. Fig. 11 (a) illustrates the PV side voltage and current, the step change response at time 0.6 s is zoomed in. Fig. 11 (b) demonstrates the output voltage of the 7 level grid connected inverter. The grid side voltage and current are illustrated in Fig. 11 (c) when the step change occurs in solar irradiance at time 0.6 s. As it is illustrated the injected current to the grid has fast dynamic response. The THD of the grid side current is about 1.8% which is within the IEEE-519 standard [32].

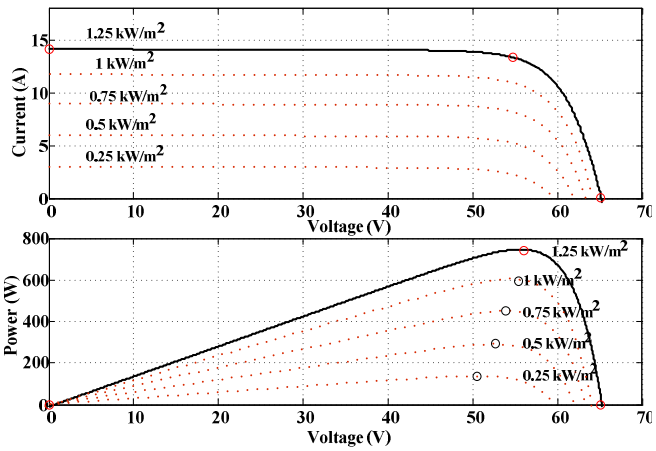

Fig. 8: I-V and P-V characteristics of the PV array.

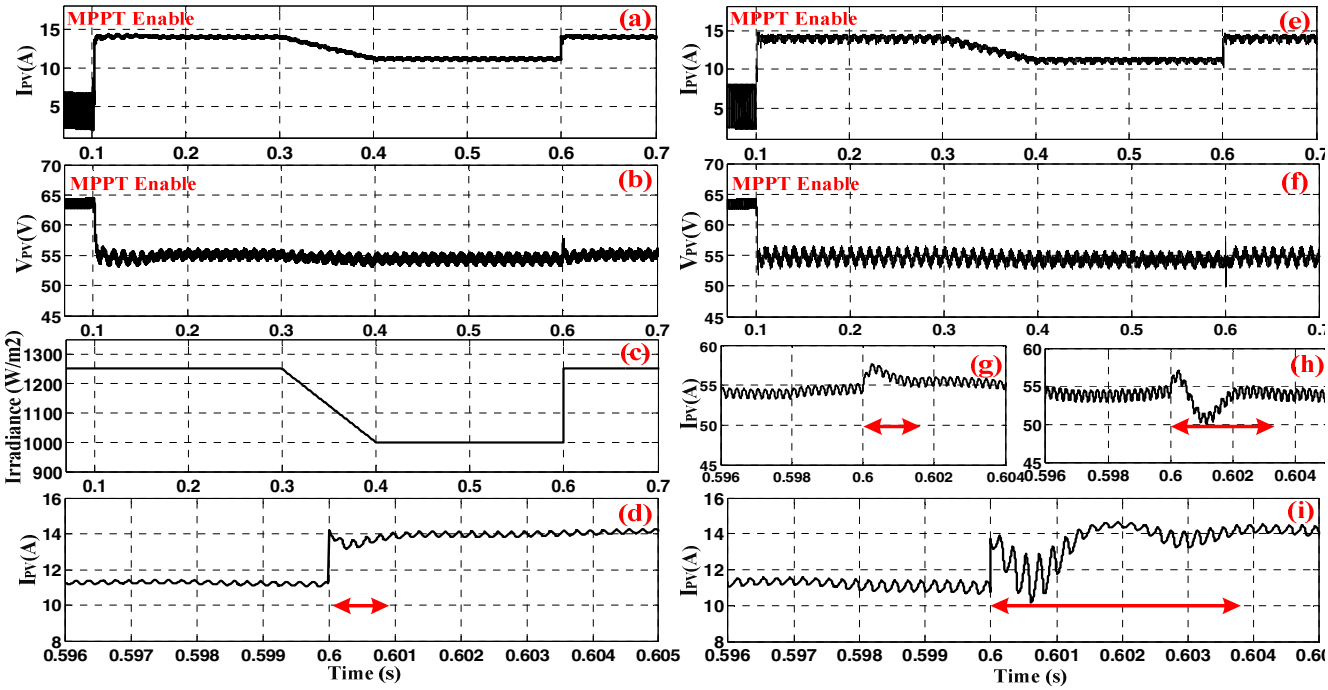

Fig. 9: a) PV current by proposed MPC-MPPT b) PV voltage by proposed MPC-MPPT c) Irradiance level d) Zoomed in plot of PV current by proposed MPC-MPPT when the step change in irradiance level at time 0.6 s occur e) PV current by INC-MPPT f) PV voltage by INC-MPPT g) Zoomed in plot of PV voltage by MPC-MPPT at time 0.6 s h) Zoomed in plot of PV voltage by INC-MPPT at time 0.6 s i) Zoomed in plot of PV current by INC-MPPT at time 0.6 s.

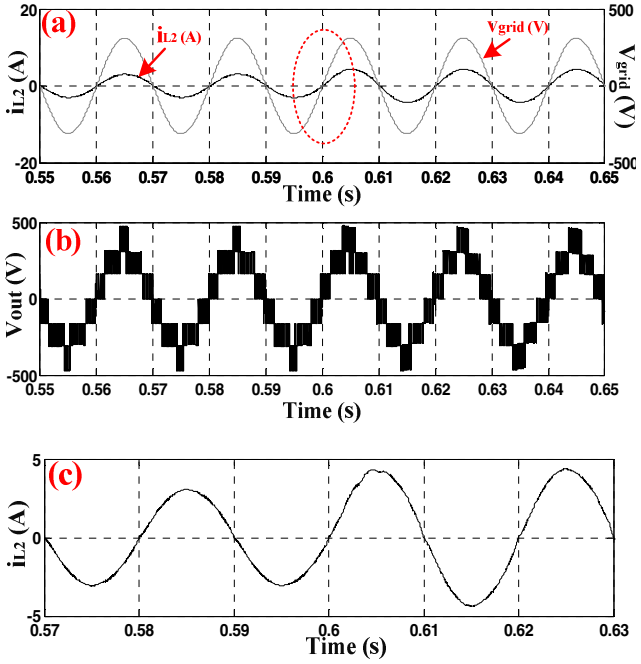

Fig. 10: a) Grid side voltage and injected current b) Output voltage of the 7 level inverter c) Zoomed in plot of the injected current to the grid by using MPC-MPPT and predictive control of 7 level inverter at time 0.6 s d) Spectrum analysis of grid side current (i_{L2})

VI. Conclusion

This paper presents an improved MPPT technique using MPC for grid connected photovoltaic systems by predicting the error at the next sampling time before applying the switching signal. The proposed two steps predictive MPPT technique is compared to the commonly used INC method to show improvement in the dynamic performance and efficiency of the MPPT. The technique exhibits fast convergence, which is ideal for rapidly varying environmental conditions such as changing temperature or insolation or changes in morphology of the PV array itself. As a result, more energy will be captured from the PV system and injected into grid particularly during partially cloudy sky without requiring expensive sensing and communications equipment and networks to directly measure the changing solar insolation.

The maximized captured energy is fed to the grid though a 7 level inverter controlled by means of predictive control. High quality current, with low THD and in-phase with the grid voltage, is achieved and injected into the grid by using the proposed predictive controller. The dSPACE DS1103 is used for implementing the control technique experimentally.

Acknowledgment

This publication was made possible by NPRP grant # 4-077-2-028 from the Qatar National Research Fund (a member of Qatar Foundation). The statements made herein are solely the responsibility of the authors.

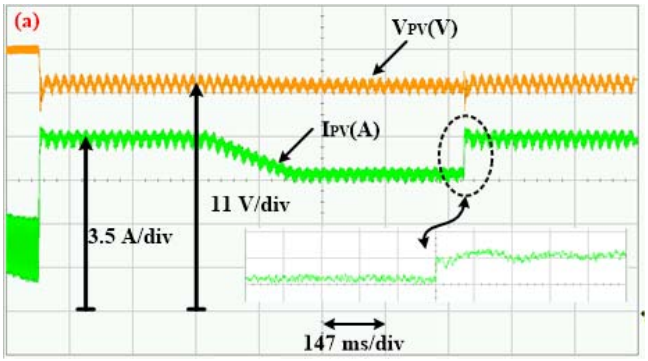

a) PV voltage and current by proposed MPC-MPPT technique

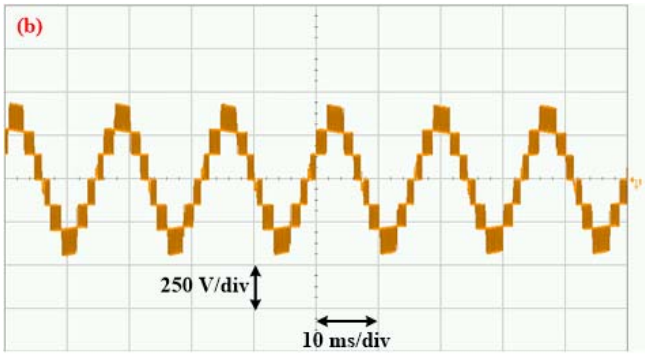

b) Output voltage of the 7 level grid connected inverter

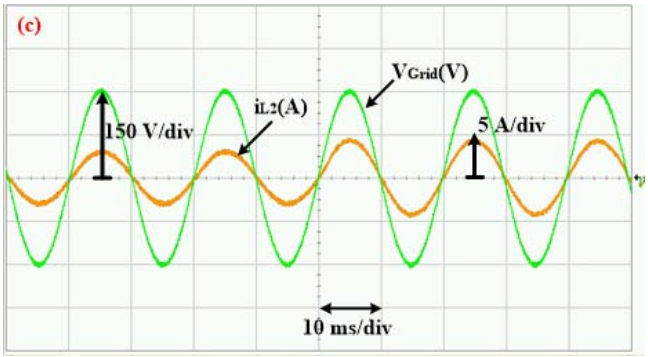

c) Grid side voltage and injected current

Fig. 11: Experimental validation of the control algorithm by real-time implementation

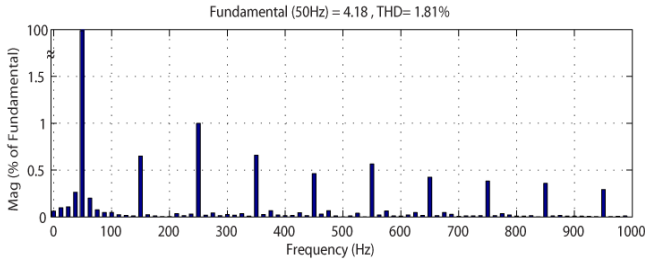

Fig. 12: Spectrum analysis of grid side current (i_{L2})

VII. REFRENCES

[1] Z. Peng, W. Yang, X. Weidong, and L. Wenyuan, "Reliability Evaluation of Grid-Connected Photovoltaic Power Systems," *IEEE Transactions on Sustainable Energy,* vol. 3, pp. 379-389, 2012.

[2] B. Fahimi, A. Kwasinski, A. Davoudi, R. S. Balog, and M. Kiani, "Charge It!," *IEEE Power and Energy Magazine,* vol. 9, pp. 54-64, 2011.

[3] S. Jie, L. Wei-jen, L. Yongqian, Y. Yongping, and P. Wang, "Forecasting Power Output of Photovoltaic Systems Based on Weather Classification and Support Vector Machines," *IEEE Transactions on Industry Applications,* vol. 48, pp. 1064-1069, 2012.

[4] D. Sera, T. Kerekes, R. Teodorescu, and F. Blaabjerg, "Improved MPPT Algorithms for Rapidly Changing Environmental Conditions," in *IEEE Power Electronics and Motion Control Conference (EPE-PEMC)*, 2006, pp. 1614-1619.

[5] M. B. Shadmand, R. S. Balog, and M. D. Johnson, "Predicting Variability of High-Penetration Photovoltaic Systems in a Community Microgrid by Analyzing High-Temporal Rate Data," *IEEE Transactions on Sustainable Energy,* vol. 5, pp. 1434-1442, 2014.

[6] A. Bidram, A. Davoudi, and R. S. Balog, "Control and Circuit Techniques to Mitigate Partial Shading Effects in Photovoltaic Arrays," *IEEE Journal of Photovoltaics,* vol. 2, pp. 532-546, 2012.

[7] T. Esram and P. L. Chapman, "Comparison of Photovoltaic Array Maximum Power Point Tracking Techniques," *IEEE Transactions on Energy Conversion,* vol. 22, pp. 439-449, 2007.

[8] P. S. Shenoy, K. A. Kim, B. B. Johnson, and P. T. Krein, "Differential Power Processing for Increased Energy Production and Reliability of Photovoltaic Systems," *IEEE Transactions on Power Electronics,* vol. 28, pp. 2968-2979, 2013.

[9] M. Shadmand, R. S. Balog, and H. Abu Rub, "Maximum Power Point Tracking using Model Predictive Control of a flyback converter for photovoltaic applications," in *IEEE Power and Energy Conference at Illinois (PECI)*, 2014, pp. 1-5.

[10] M. B. Shadmand, M. Mosa, R. S. Balog, and H. A. Rub, "An Improved MPPT Technique of High Gain DC-DC Converter by Model Predictive Control for Photovoltaic Applications," in *IEEE Applied Power Electronics Conference & Exposition (APEC)*, 2014, pp. 2993 - 2999.

[11] A. R. Kashyap, R. Ahmadi, and J. W. Kimball, "Input voltage control of SEPIC for maximum power point tracking," in *IEEE Power and Energy Conference at Illinois (PECI)*, 2013, pp. 30-35.

[12] H. Zhang and R. S. Balog, "Experimental Verification of Energy Harvest from Non-Planar Photovoltaic Surfaces," in *Energy Conversion Congress and Exposition (ECCE)*, Denver, CO, USA 2013, pp. 4481 - 4487.

[13] M. B. Shadmand and R. S. Balog, "Mitigating Variability of High Penetration Photovoltaic Systems in a Community Smart Microgrid using Non-Flat Photovoltaic Modules," in *Energy Conversion Congress and Exposition (ECCE)*, Denver, CO, USA, 2013, pp. 554 - 560.

[14] A. Karavadi and R. S. Balog, "Novel non-Flat PV Module Geometries and Implications to Power Conversion," in *Energy Conversion Congress and Exposition (ECCE)*, Phoenix, AZ, 2011, pp. 7-13.

[15] N. Femia, G. Petrone, G. Spagnuolo, and M. Vitelli, "Optimization of perturb and observe maximum power point tracking method," *IEEE Transactions on Power Electronics,* vol. 20, pp. 963-973, 2005.

[16] K. A. Kim, R. M. Li, and P. T. Krein, "Voltage-offset resistive control for DC-DC converters in photovoltaic applications," in *IEEE Applied Power Electronics Conference and Exposition (APEC)*, 2012, pp. 2045-2052.

[17] S. Harb, H. Zhang, and R. S. Balog, "AC-link, single-phase, photovoltaic Module Integrated Inverter," in *IEEE Applied Power Electronics Conference and Exposition (APEC)*, 2013, pp. 177-182.

[18] H. Keyhani, H. A. Toliyat, M. H. Todorovic, R. Lai, and R. Datta, "A Step-Up/Down Three-Phase Resonant High-Frequency AC-Link Inverter," in *IEEE Applied Power Electronics Conference and Exposition (APEC)*, 2013.

[19] R. Ahmadi, A. Kashyap, A. Berrueta Irigoyen, A. Rayachoti, C. Wright, and J. Kimball, "Selective source power converter for improved photovoltaic power utilization," in *IEEE Power and Energy Conference at Illinois (PECI)*, 2013, pp. 247-252.

[20] A. Amirahmadi, C. Lin, U. Somani, H. Haibing, N. Kutkut, and I. Bartarseh, "High Efficiency Dual-Mode Current Modulation Method for Low-Power DC/AC Inverters," *IEEE Transactions on Power Electronics,* vol. 29, pp. 2638-2642, 2014.

[21] B. Farhangi and S. Farhangi, "Comparison of z-source and boost-buck inverter topologies as a single phase transformer-less photovoltaic grid-connected power conditioner," in *IEEE Power Electronics Specialists Conference (PESC)*, 2006, pp. 1-6.

[22] M. Hamzeh, S. Farhangi, and B. Farhangi, "A new control method in PV grid connected inverters for anti-islanding protection by impedance monitoring," in *IEEE Workshop on Control and Modeling for Power Electronics (COMPEL)*, 2008, pp. 1-5.

[23] S. Sajadian and E. C. dos Santos, "Three-phase DC-AC converter with five-level four-switch characteristic," in *Power and Energy Conference at Illinois (PECI)*, 2014, pp. 1-6.

[24] E. C. dos Santos Junior and S. Sajadian, "Energy conversion unit with optimized waveform generation," in *IEEE Industry Applications Society Annual Meeting*, 2013, pp. 1-6.

[25] D. Maksimovic and S. Cuk, "Switching converters with wide DC conversion range," *IEEE Transactions on Power Electronics,* vol. 6, pp. 151-157, 1991.

[26] J. Holtz and S. Stadtfeld, "A predictive controller for the stator current vector of AC machines fed from a switched voltage source," in *International Power Electronics Conference (IPEC)*, 1983, pp. 1665–1675.

[27] J. Rodriguez and P. Cortes, *Predictive control of power converters and electrical drives* vol. 37: John Wiley & Sons, 2012.

[28] J. Rodriguez, M. P. Kazmierkowski, J. R. Espinoza, P. Zanchetta, H. Abu-Rub, H. A. Young*, et al.*, "State of the Art of Finite Control Set Model Predictive Control in Power Electronics," *IEEE Transactions on Industrial Informatics,* vol. 9, pp. 1003-1016, 2013.

[29] H. Abu-Rub, J. Guzinski, Z. Krzeminski, and H. A. Toliyat, "Predictive current control of voltage-source inverters," *IEEE Transactions on Industrial Electronics,* vol. 51, pp. 585-593, 2004.

[30] P. Cortes, A. Wilson, S. Kouro, J. Rodriguez, and H. Abu-Rub, "Model Predictive Control of Multilevel Cascaded H-Bridge Inverters," *IEEE Transactions on Industrial Electronics,* vol. 57, pp. 2691-2699, 2010.

[31] J. D. Barros, J. F. A. Silva, and E. G. A. Jesus, "Fast-Predictive Optimal Control of NPC Multilevel Converters," *IEEE Transactions on Industrial Electronics,* vol. 60, pp. 619-627, 2013.

[32] C. K. Duffey and R. P. Stratford, "Update of harmonic standard IEEE-519: IEEE recommended practices and requirements for harmonic control in electric power systems," *IEEE Transactions on Industry Applications,* vol. 25, pp. 1025-1034, 1989.